Increasing Mobility and Spin Lifetime with Shear Strain in Thin Silicon Films

Dmitri Osintsev, Viktor Sverdlov, Thomas Windbacher, and Siegfried Selberherr
Institute for Microelectronics, TU Wien, Gußhausstraße 27–29/E360, A–1040 Wien, Austria
Email: {osintsev | sverdlov | selberherr}@iue.tuwien.ac.at

***Abstract*—Because of an ongoing shift to FinFETs/ultra-thin body SOI based devices for the 22nm node and beyond, mobility enhancement in such structures is an important issue. Stress engineering used by the semiconductor industry to boost mobility was predicted to become less efficient in ultra-thin SOI structures due to the less pronounced dependence of the transport effective mass on strain. Using the $\mathbf{k}\cdot\mathbf{p}$ Hamiltonian which accurately describes the wave functions of electrons in silicon in the presence of strain and spin-orbit interaction, we show that the wave functions and the matrix elements' dependences on strain compensate the weaker dependence of the effective mass, which results in an almost two-fold mobility increase even in ultra-thin (001) SOI films under tensile [110] stress. In addition, we demonstrate that the spin relaxation rate due to surface roughness and phonon scattering is also efficiently suppressed by an order of magnitude by applying tensile stress, which makes SOI structures attractive for spin-driven applications.**

I. Introduction

Resent advances in semiconductor device scaling and development of multi-core processor architectures have continuously boosted the performance enhancement of modern computers. Ongoing miniaturization of microelectronic devices makes the developement of accurate transport models in ultra-thin body SOI MOSFETs and finFETs paramount. Mobility enhancement in such structures is an important issue. Stress is routinely used to enhance the carrier mobility, However, it is expected that in ultra-thin SOI structures stress becomes less efficient for this purpose [1].

With both, scaling and multi-core approaches, showing signs of saturation a new development benefiting from the three-dimensional (3D) integration technology of the components and circuits will allow to extend Moore's law by putting more transistors on a die. However, to proceed with the performance enhancement beyond 3D integration the development of conceptually new innovative approaches is mandatory.

Electron spin attracts a significant attention lately [2]. Spintronics is a rapidly developing and promising technology exploiting spin properties of electrons. A number of potential spintronic devices has been proposed. Silicon, the main element of microelectronics, is also promising for spin-driven applications [2], because it is composed of nuclei with predominantly zero spin and is characterized by small spin-orbit coupling. Both factors favour to reduce the spin relaxation. However, the experimentally observed enhancement of spin relaxation in electrically gated lateral-channel silicon structures [3] could compromise the reliability and become an obstacle in realizing spin-driven devices. Deeper understanding of scattering and spin relaxation mechanisms in thin silicon films is therefore needed.

We investigate the surface roughness and electron-phonon limited electron mobility and spin relaxation in silicon films under shear strain. We show that due to the usually neglected dependence of the surface roughness scattering matrix elements on strain the electron mobility in such structures shows a two times increase with strain. Shear strain also results in a degeneracy lifting between the unprimed subbands resulting in a spin lifetime increase by at least an order of magnitude.

II. Model

In order to find the corresponding scattering matrix elements, the subband structure and the wave functions in silicon films must be calculated. For this purpose the effective $\mathbf{k}\cdot\mathbf{p}$ Hamiltonian describing the electron states in the conduction band of the two relevant [001] valleys in presence of shear strain ε_{xy}, spin-orbit interaction, and confinement potential $U(z)$ is written in the vicinity of the X-point along the k_z-axis in the Brillouin zone as [4], [5]

$$H=\begin{bmatrix} H_1 & H_3 \\ H_3^\dagger & H_2 \end{bmatrix}, \tag{1}$$

with H_1, H_2, and H_3 as

$$H_1=\begin{bmatrix} 1 & 0 \\ 0 & 1 \end{bmatrix}\times\left(\frac{\hbar^2k_z^2}{2m_l}+\frac{\hbar^2\left(k_x^2+k_y^2\right)}{2m_t}-\frac{\hbar^2k_0k_z}{m_l}+U(z)\right), \tag{2}$$

$$H_2=\begin{bmatrix} 1 & 0 \\ 0 & 1 \end{bmatrix}\times\left(\frac{\hbar^2k_z^2}{2m_l}+\frac{\hbar^2\left(k_x^2+k_y^2\right)}{2m_t}+\frac{\hbar^2k_0k_z}{m_l}+U(z)\right), \tag{3}$$

$$H_3=\begin{bmatrix} D\varepsilon_{xy}-\frac{\hbar^2k_xk_y}{M} & (k_y-k_x\mathrm{i})\,\Delta_{so} \\ (-k_y-k_x\mathrm{i})\,\Delta_{so} & D\varepsilon_{xy}-\frac{\hbar^2k_xk_y}{M} \end{bmatrix}. \tag{4}$$

$M^{-1}\approx m_t^{-1}-m_0^{-1}$, D =14eV is the shear strain deformation potential, Δ_{so} =1.27meVnm, m_t and m_l are the transversal and the longitudinal silicon effective masses, k_0 =0.15×2π/a is the position of the valley minimum relative to the X-point in unstrained silicon. The unprimed subband energies and the four component wave functions are used to evaluate the scattering matrix elements and rates. The primed subbands can be described in a similar fashion [1].

The $\mathbf{k}\cdot\mathbf{p}$ approach [1], [4], [5] is suitable to describe the electron subband structure and to find the wave functions in (001) silicon films in analytical form both in presence of strain and spin-orbit interaction provided the confinement potential is approximated by an infinite square well. The same formalism can be employed to find the wave functions for

978-1-4799-5288-5/14/$31.00

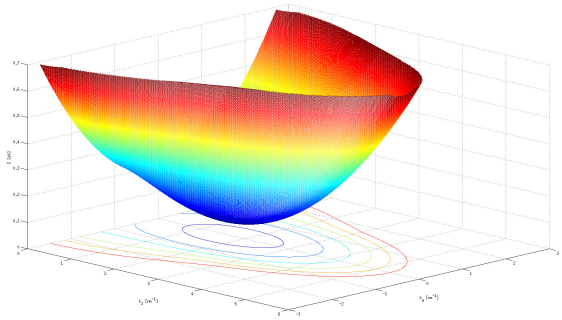

Fig. 1. The primed subband dispersion in the 6nm thick film. The transverse mass m_t is close to its value in bulk Si m_t=0.19m_0.

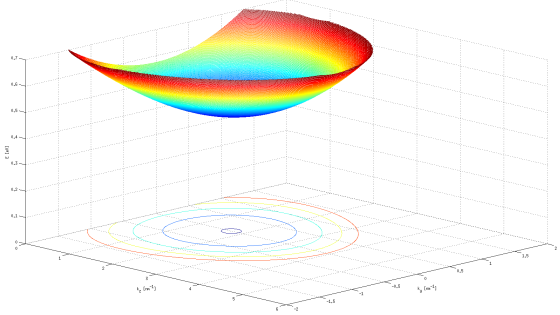

Fig. 2. The primed subband dispersion in the film of 2 nm thickness. The transverse mass has increased with the thickness reduced.

primed subbands [1]. In Fig. 1 and Fig. 2 the dispersion of the first unprimed subbands in films of thicknesses 6nm and 2.1nm, respectively, is compared. The effective mass m_l = 0.91 m_0 along the OZ-direction does not depend on the thickness. In sharp contrast, the effective mass m_t along the OX-direction shows a strong increase as the film thickness decreases, in agreement with earlier predictions [1].

III. Momentum and Spin Relaxation Rates

We are considering the surface roughness (SR) and electron-phonon scattering mechanisms contributing to the spin and momentum relaxation.

The spin and momentum relaxation times are calculated by thermal averaging of the corresponding subbands' in-plane momentum $\mathbf{K}_i$ dependent scattering rates $\tau_i(\mathbf{K}_i)$ [4], [6] as

$$\frac{1}{\tau} = \frac{\sum_i \int \frac{1}{\tau_i(\mathbf{K}_i)} f(E_i)\left(1 - f(E_i)\right) d\mathbf{K}_i}{\sum_i \int f(E_i)\, d\mathbf{K}_i}, \tag{5}$$

$$\int d\mathbf{K}_i = \int_0^{2\pi} \int_{E_i^{(0)}}^{\infty} \frac{\mathbf{K}_i}{\left|\frac{\partial E_i}{\partial \mathbf{K}_i}\right|} d\varphi dE. \tag{6}$$

Here $f(E) = \left[1 + \exp\left((E - E_F)/k_B T\right)\right]^{-1}$, where k_B is the Boltzmann constant, T is the temperature, E_F is the Fermi energy, $E = E_i^{(0)} + E_i(\mathbf{K}_i)$, $E_i^{(0)} = E_i(\mathbf{K}_i = 0)$ is the energy of the bottom of the subband i, and

$$\left|\frac{\partial E_i}{\partial \mathbf{K}_i}\right| = \left|\frac{\partial E(\mathbf{K}_i)}{\partial \mathbf{K}_i}\right|_{\varphi, E}, \tag{7}$$

is the derivative of the subband dispersion along $\mathbf{K}_i$ at the angle φ defining the $\mathbf{K}_i$ direction. The surface roughness momentum (spin) relaxation rate in the subband i is calculated in the following way [6]:

$$\frac{1}{\tau_i^{SR}(\mathbf{K}_i)} = \frac{2(4)\pi}{\hbar (2\pi)^2} \sum_j \int_0^{2\pi} \pi \Delta^2 L^2 \frac{1}{\epsilon_{ij}^2 (\mathbf{K}_i - \mathbf{K}_j)} \frac{\hbar^4}{4 m_l^2} \frac{|\mathbf{K}_j|}{\left|\frac{\partial E(\mathbf{K}_j)}{\partial \mathbf{K}_j}\right|} \cdot$$
$$\cdot \left[\left(\frac{d\Psi_{i\mathbf{K}_i\sigma(-\sigma)}}{dz}\right)^* \left(\frac{d\Psi_{j\mathbf{K}_j\sigma}}{dz}\right)\right]_{z=\pm\frac{t}{2}}^2 \cdot$$
$$\cdot \exp\left(\frac{-(\mathbf{K}_j - \mathbf{K}_i) L^2}{4}\right) d\varphi. \tag{8}$$

$\mathbf{K}_i, \mathbf{K}_j$ are the in-plane wave vectors before and after scattering, φ is the angle between $\mathbf{K}_i$ and $\mathbf{K}_j$, ϵ is the dielectric permittivity, L is the autocorrelation length, Δ is the mean square value of the surface roughness fluctuations, $\Psi_{i\mathbf{K}_i}$ and $\Psi_{j\mathbf{K}_j}$ are the wave functions, and $\sigma = \pm 1$ is the spin projection to the [001] axis.

The intervalley spin relaxation rate contains the Elliott and Yafet contributions, which are calculated in the following way:

$$\frac{1}{\tau_i^{LA}(\mathbf{K}_i)} = \frac{k_B T}{\hbar \rho \upsilon_{LA}^2} \sum_j \int_0^{2\pi} \frac{|\mathbf{K}_j|}{\left|\frac{\partial E(\mathbf{K}_j)}{\partial \mathbf{K}_j}\right|} \left[1 - \frac{\left|\frac{\partial E(\mathbf{K}_j)}{\partial \mathbf{K}_j}\right| f(E(\mathbf{K}_j))}{\left|\frac{\partial E(\mathbf{K}_i)}{\partial \mathbf{K}_i}\right| f(E(\mathbf{K_i}))}\right] \cdot$$
$$\cdot \int_0^t \left[\Psi_{j\mathbf{K}_j-\sigma}^{\dagger}(z)\, M' \Psi_{i\mathbf{K}_i\sigma}(z)\right]^* \cdot$$
$$\cdot \left[\Psi_{j\mathbf{K}_j-\sigma}^{\dagger}(z')\, M' \Psi_{i\mathbf{K}_i\sigma}(z')\right] dz d\varphi. \tag{9}$$

Here the matrix M' is written as

$$M' = \begin{bmatrix} M_{ZZ} & M_{SO} \\ M_{SO}^{\dagger} & M_{ZZ} \end{bmatrix}, \tag{10}$$

$$M_{ZZ} = \begin{bmatrix} \Xi & 0 \\ 0 & \Xi \end{bmatrix}, \tag{11}$$

$$M_{SO} = \begin{bmatrix} 0 & D_{SO}(r_y - i r_x) \\ D_{SO}(-r_y - i r_x) & 0 \end{bmatrix}, \tag{12}$$

where $\Xi = 12$eV is the acoustic deformation potential, $(r_y, r_x) = \mathbf{K}_i + \mathbf{K}_j$, and $D_{SO} = 15\text{meV}/k_0$ with $k_0 = 0.15 \cdot 2\pi/a$ defined as the position of the valley minimum relative to the X-point in unstrained silicon. In contrast to mobility calculations, when the main contribution to (8) and (9) is due to intrasubband scattering, the spin relaxation is mostly determined by intersubband transitions.

Intrasubband transitions are important for the contributions determined by the shear deformation potential. The spin relaxation rate due to the transversal acoustic phonons is calculated

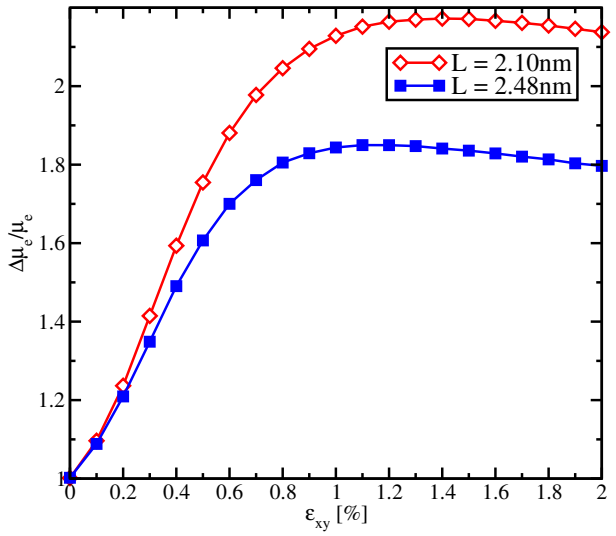

Fig. 3. Electron mobility enhancement as a function of strain for electron concentration N_S=2.6·10^{12}cm^{-2} at room temeparture.

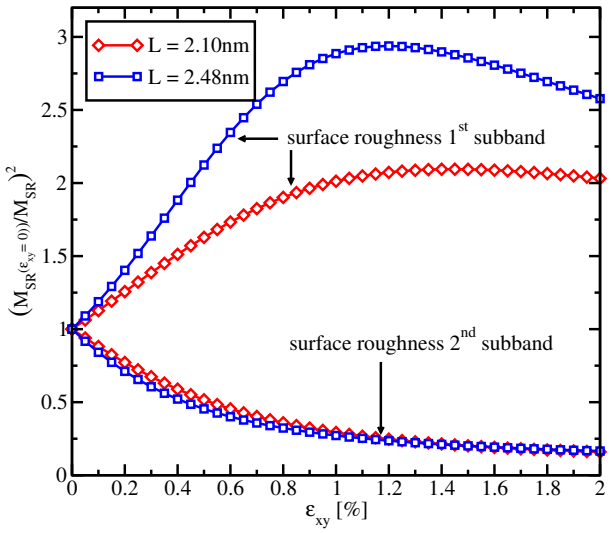

Fig. 4. Dependence of the inversed normalized square of surface roughness intrasubband matrix elements for different film thicknesses.

as [5]

$$\frac{1}{\tau_i^{TA}(\mathbf{K}_i)} = \frac{k_B T}{\hbar\rho\upsilon_{TA}^2}\sum_j\int_0^{2\pi}\frac{|\mathbf{K}_j|}{\left|\frac{\partial E(\mathbf{K}_j)}{\partial \mathbf{K}_j}\right|}\cdot \left[1-\frac{\left|\frac{\partial E(\mathbf{K}_j)}{\partial \mathbf{K}_j}\right| f(E(\mathbf{K}_j))}{\left|\frac{\partial E(\mathbf{K}_i)}{\partial \mathbf{K}_i}\right| f(E(\mathbf{K_i}))}\right]\cdot \int_0^t\int_0^t \exp\left(-\sqrt{q_x^2+q_y^2}\,|z-z'|\right)\cdot \left[\Psi^\dagger_{j\mathbf{K}_j-\sigma}(z)\,M\Psi_{i\mathbf{K}_i\sigma}(z)\right]^*\left[\Psi^\dagger_{j\mathbf{K}_j-\sigma}(z')\,M\Psi_{i\mathbf{K}_i\sigma}(z')\right]\cdot \left[\sqrt{q_x^2+q_y^2}-\frac{8q_x^2q_y^2-\left(q_x^2+q_y^2\right)^2}{q_x^2+q_y^2}\,|z-z'|\right]dzdz'd\varphi, \tag{13}$$

where ρ=2329$\frac{kg}{m^3}$ is the silicon density, υ_{TA}=5300$\frac{m}{s}$ is the transversal phonons′ velocity, $(q_x, q_y) = \mathbf{K}_i - \mathbf{K}_j$, and M is the 4×4 matrix written in the basis for the spin relaxation rate.

$$M = \begin{bmatrix} 0 & 0 & D/2 & 0 \\ 0 & 0 & 0 & D/2 \\ D/2 & 0 & 0 & 0 \\ 0 & D/2 & 0 & 0 \end{bmatrix}. \tag{14}$$

Here D=14eV is the shear deformation potential.

The intravalley spin relaxation rate due to longitudinal acoustic phonons is calculated as [5]

$$\frac{1}{\tau_i^{LA}(\mathbf{K}_i)} = \frac{k_B T}{\hbar\rho\upsilon_{LA}^2}\sum_j\int_0^{2\pi}\frac{|\mathbf{K}_j|}{\left|\frac{\partial E(\mathbf{K}_j)}{\partial \mathbf{K}_j}\right|}\left[1-\frac{\left|\frac{\partial E(\mathbf{K}_j)}{\partial \mathbf{K}_j}\right| f(E(\mathbf{K}_j))}{\left|\frac{\partial E(\mathbf{K}_i)}{\partial \mathbf{K}_i}\right| f(E(\mathbf{K_i}))}\right]\cdot \int_0^t\int_0^t \exp\left(-\sqrt{q_x^2+q_y^2}\,|z-z'|\right)\cdot \left[\Psi^\dagger_{j\mathbf{K}_j-\sigma}(z)\,M\Psi_{i\mathbf{K}_i\sigma}(z)\right]^*\left[\Psi^\dagger_{j\mathbf{K}_j-\sigma}(z')\,M\Psi_{i\mathbf{K}_i\sigma}(z')\right]\cdot \frac{4q_x^2q_y^2}{\left(\sqrt{q_x^2+q_y^2}\right)^3}\left[\sqrt{q_x^2+q_y^2}\,|z-z'|+1\right]dzdz'd\varphi. \tag{15}$$

Here υ_{LA}=8700$\frac{m}{s}$ is the speed of the longitudinal phonons and the matrix is defined with (14).

The momentum relaxation time is evaluated in the standard way [6]. The electron mobility in inversion layers in [110] direction is calculated as [6]

$$\mu_{110} = \frac{e}{4\pi^2\hbar^2 k_B T n_s}\sum_i\int_0^{2\pi}d\phi\int_{E_i^{(0)}}^{\infty}dE\frac{|\mathbf{K}_i|}{\left|\frac{\partial E(\mathbf{K}_i)}{\partial \mathbf{K}_i}\right|}\cdot \left(\frac{\partial E(\mathbf{K}_i)}{\partial \mathbf{K}_i}\right)^2_{\varphi=\pi/4,E}\tau_{110}^{(i)}f(E)\left(1-f(E)\right), \tag{16}$$

where $n_s = \sum_i n_i$, n_i is the population of subband i, and $\tau_{110}^{(i)}$ is the momentum relaxation time in subband i for [110] direction.

IV. Results

Fig. 3 shows the electron mobility enhancement in [110] direction along tensile stress as a function of shear strain. Our results show that the mobility in thin silicon films increases by a factor of two. The increase depends on the film thickness. For the thicknesses considered a strong mobility enhancement is observed up to a shear strain value around 0.5%. When

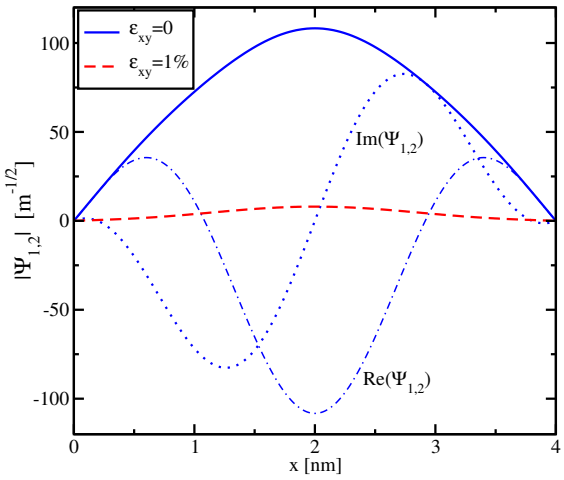

Fig. 5. The small spin-down component responsible for spin relaxation is significantly reduced by shear strain.

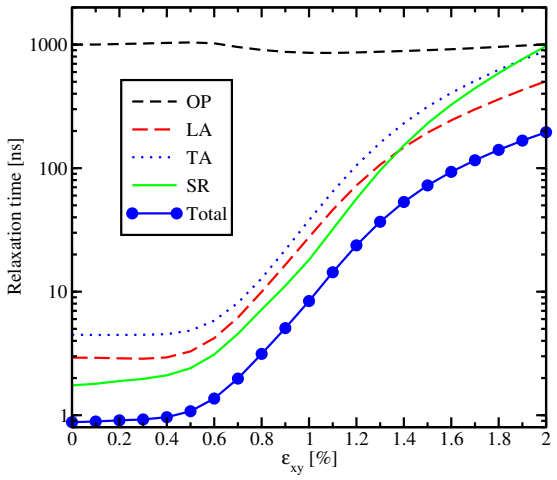

Fig. 6. Spin lifetime enhancement by shear strain in a 2.48nm thin silicon film. Contributions due to optical, acoustic, and SR are included.

the shear strain is further increased, the mobility saturates and even shows a slight decrease for the film thicknesses 2.1nm and 2.48nm, respectively.

The [110] mobility enhancement in surface layers due to tensile stress applied along the channel is usually explained by the effective transport mass reduction. However, the effective mass decrease in the lowest subband can only account for roughly one half of the mobility enhancement obtained and cannot explain the two-fold mobility enhancement. Thus, more analysis is needed to understand the effect.

The inverse SR scattering matrix elements are shown in Fig. 4. The decrease of the scattering matrix elements with shear strain accounts for the remaining 50% of the total mobility enhancement observed in Fig. 3. For the t=2.1nm film the unaccounted mobility enhancement is mostly due to the SR mobility increase. Although the SR mobility growths stronger for t=2.48nm, the main contribution to limit the mobility is phonon scattering. For this reason the whole mobility for t=2.48nm is slightly less enhanced as compared to that in the t=2.1nm film.

Because the spin-orbit interaction involves the electron spin, the spin-up wave function is not the eigenstate of the Hamiltonian. Therefore, the wave function always contains a small but finite component corresponding to the spin-down component. Fig. 5 shows the spin-down component in a valley along [001] direction. Analyzing the wave function components' absolute value and its real and imaginary parts one concludes that it is well described by the quantization envelope function $\sin(\pi z/t)$ times the phase factor $\exp(\pm ik_0 z)$, where k_0 describes the valley minimum position relative to the X-point in the Brillouin zone. Importantly, when shear strain is applied, the amplitude of the spin-down component is significantly reduced.

Because the value of this component determines the strength of the Elliot contribution to spin relaxation [4], shear strain can be used to boost the spin lifetime in ultra-thin body SOI MOSFETs. The spin lifetime enhancement by shear strain is shown in Fig. 6. Here the spin relaxation induced by the surface roughness and longitudinal acoustic phonon scattering between the [001] valleys and transversal acoustic intravalley scattering are included. A substantial spin lifetime enhancement is observed. It is mediated by the shear strain induced splitting between the [001] valleys [1]. In addition, we have included the spin relaxation contribution due to phonon scattering between non-equivalent valleys (f-type intervalley scattering). The later gives the main contribution to the spin relaxation in bulk silicon [4]. In thin films this mechanism is less important due to the large confinement induced splitting between the primed and unprimed subbands.

V. Conclusion

We have presented an approach to evaluate mobility and spin lifetime in strained ultra-thin silicon films. We have shown that the usually neglected surface roughness matrix scattering elements' dependence on strain makes it possible to double the electron mobility in stressed thin silicon films. We have demonstrated a strong, almost two orders of magnitude, increase of spin lifetime in strained silicon films. Thus shear strain used to boost mobility can also be used to increase spin lifetime.

Acknowledgment

This work is supported by the European Research Council through the grant #247056 MOSILSPIN. The computational results have been achieved in part using the Vienna Scientific Cluster (VSC).

References

[1] V. Sverdlov. Strain-induced Effects in Advanced MOSFETs. Springer 2011.

[2] R. Jansen, "Silicon Spintronics," *Nat.Mater.*, vol. 11, p. 400, 2012.

[3] J. Li and I. Appelbaum, "Modeling Spin Transport in Electrostatically-gated Lateral-channel Silicon Devices: Role of Interfacial Spin Relaxation," *Phys.Rev. B*, vol. 84, p. 165318, 2011.

[4] P. Li and H. Dery, "Spin-orbit Symmetries of Conduction Electrons in Silicon," *Phys.Rev.Lett.*, vol. 107, p. 107203, 2011.

[5] D. Osintsev, V. Sverdlov, and S. Selberherr, "Reduction of Momentum and Spin Relaxation Rate in Strained Thin Silicon Films", *Proc. of the 43rd ESSDERC*, p. 334. 2013.

[6] M.V. Fischetti et al., "Six-band k·p Calculation of the Hole Mobility in Silicon Inversion Layers: Dependence on Surface Orientation, Strain, and Silicon Thickness," *J.Appl.Phys.*, vol. 94, p. 1079, 2003.